Universität Freiburg
Advanced Physics Lab Course
FP1 2024-2

Experiment 1
Cosmic Muons

Short Report

[redacted]

September 19, 2024

Lab Work conducted: September 16 & 17

Assistant: [redacted]

Contents

1 Objectives

This experiment is dedicated to measuring the flux Φ of cosmic muons reaching the surface of the earth. Cosmic muons originate in decays of secondary cosmic ray shower particles like charged pions. A series of sub-experiments was performed using a setup consisting of two detector tiles and a coincidence module. Initially, measurements were conducted to assess the shape of the underlying probability density function, as well as the rate of random coincidences. After this, the zenith angle dependence of the incoming particle flux was analysed at three different locations in the buildings, corresponding to varying levels of shielding. Different statistical and systematic uncertainties were taken into account and from the measurements the total flux through a horizontal detector was estimated. Finally, the shielding effect of lead blocks brought between the two detector tiles was examined.

2 Setup and Procedure

In this experiment, an experimental kit of *CAEN Educational* [Edua] was used, which consists of two encased plastic scintillator tiles, SiPM diodes working in Geiger-Müller regime and a coincidence module, which can be read out and controlled via a software on a computer. The photodiodes as well as some electronics are enclosed in the detector tiles and their settings and bias voltage cannot be changed. When operating in coincidence mode, the two tiles can be mounted onto a metal arm which can be rotated around its point of suspension in the direction of the zenith angle Θ, forming a "muon telescope". A picture of this telescope setup can be found in fig. 1

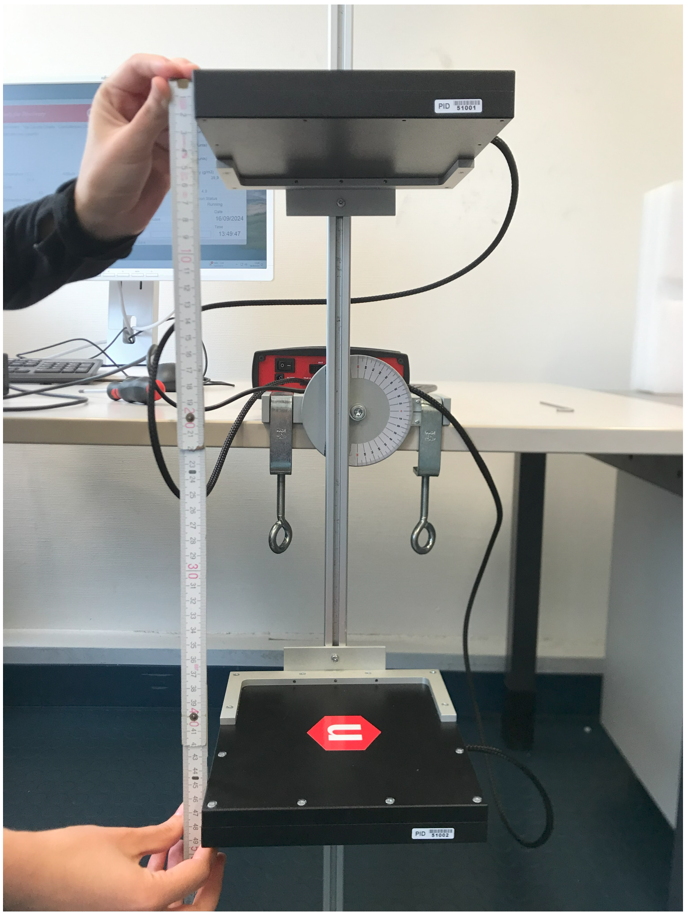

Figure 1: Setup of the muon telescope, indicating the procedure for measuring the distance d between the tiles.

For determining the underlying probability distribution, the number of coincidences detected within a time interval of 1 min and 5 s was measured repeatedly in order to obtain a statistical significance and a histogram of the results was obtained and analysed.

At three chosen locations, namely the highest floor on the physics highrise (at around 218 m of altitude), a laboratory on the first floor ($\approx$ 186 m) as well as the second basement ($\approx$ 174 m), the

dependence of the rate of measured coincidences on the zenith angle Θ was examined by measuring the coincidence rate R_c at a few different angles and taking into account the geometry of the setup, which determines the solid angle Ω. An especially long measurement for the flux at $\Theta = 0^\circ$ was conducted over night in the lab.
For estimating the rate of random coincidences, an additional measurement was performed at all the above named locations, during which the two tiles were removed from the telescope arm and placed on opposite ends of a table. The rates measured in the individual tiles at any measurement were taken into account as well.
On the highrise, a further measurement was performed, during which the distance between the two detector tiles was decreased step-wise at a constant angle and the resulting coincidence rate was noted.
Finally, we performed a few measurements during which we placed increasing thicknesses of lead blocks between the two detector tiles and observed the effect this had on the measured coincidence rate.

3 Observations & Data Analysis

3.1 Analysis: Probability Distribution

The raw data from this part of the experiment can be found in *Table 1* and *Table 6* of the lab notes in Appendix A section 6. The experiment was performed twice, first with an integration time of 1 min and later with an integration time of 5 s.
As the cosmic muons detected on earth stem from particle decays with characteristically low count rates, one would typically expect their detection rates to follow a Poisson distribution. When looking at the histogram obtained from a repeated measurement of the number of coincidences during a 5 s interval (see fig. 3), this reassembles indeed the expected slightly asymmetric shape, however it looks more like a Gaussian curve for the measurement with the longer integration time (fig. 2). In order to confirm the underlying probability density distribution, we fit a Poisson distribution

$$P_{\text{Poisson}}(N) = A \cdot \frac{\mu^N}{N!} \cdot e^{-\mu} \tag{1}$$

to the histograms, where N is the number of detected events, μ the average value and A a scaling factor. A and μ are the free parameters of the fit.
Additionally, we also fit a Gaussian distribution of the shape

$$P_{\text{Gauß}}(N) = A \cdot \frac{1}{\sqrt{2\,\pi\,\sigma^2}} \cdot e^{-\frac{(N-\mu)^2}{\sigma^2}}, \tag{2}$$

where the three free parameters are the standard deviation σ, the central value μ and again a scaling factor A. The fits were performed in python using the module *scipy.optimize.curvefit* and assuming an error of $\sqrt{P}$ on the number of counts in each bin. The results of the fits are shown in figs. 2 and 3.

As a mean of assessing the goodness of the fits, the reduced χ^2

$$\frac{\chi^2}{dof} = \frac{\sum_i \frac{(P_i - P_{\text{fit}})^2}{s_\text{i}^2}}{dof}$$

was calculated and quoted in the legends of the plots, along with the best fit parameter values and their uncertainties.

As one can see from the reduced χ^2, which has an expectancy value of 1, in the measurement with the longer integration time the data can be described just as well by a Gaussian function as by a Poisson function. This made us think that we had potentially chosen the integration time a bit too long. We know that in the limit of very high count rates, a Poisson distribution is expected to transition into a Gaussian distribution. Consequently, we decided to repeat the measurement with a shorter integration time, the result of which can be seen in fig. 3. This second histogram is described much better by a Poisson than by a Gaussian distribution, thus confirming the general expected statistical character of the muon detection.

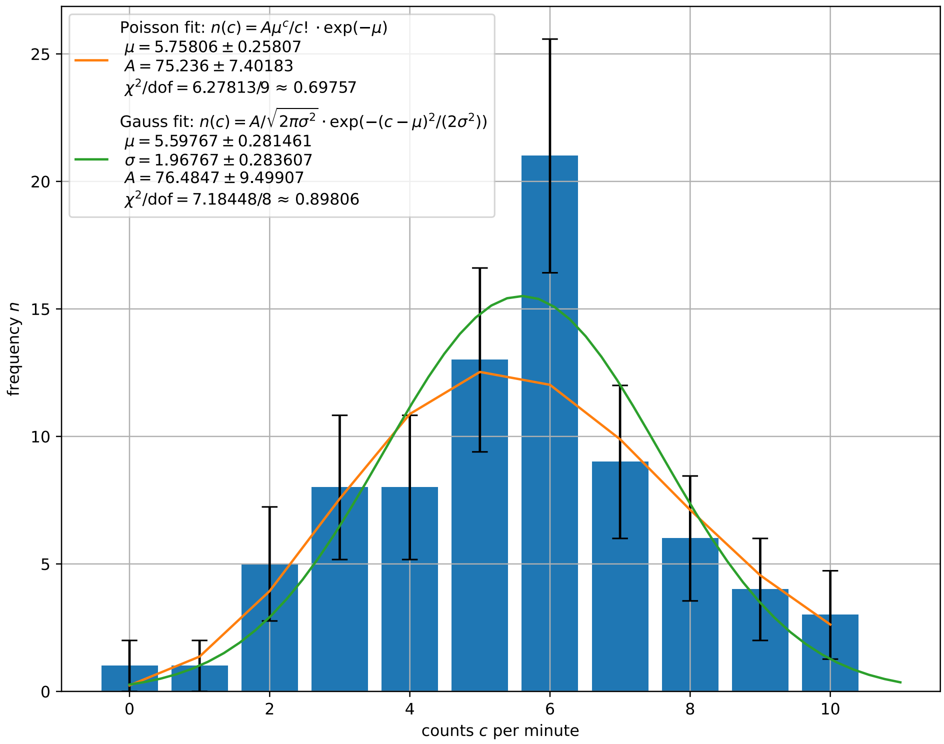

Figure 2: Probability distribution of the coincidence counts. Measured in the first floor lab with 79 measurements, 1min each.

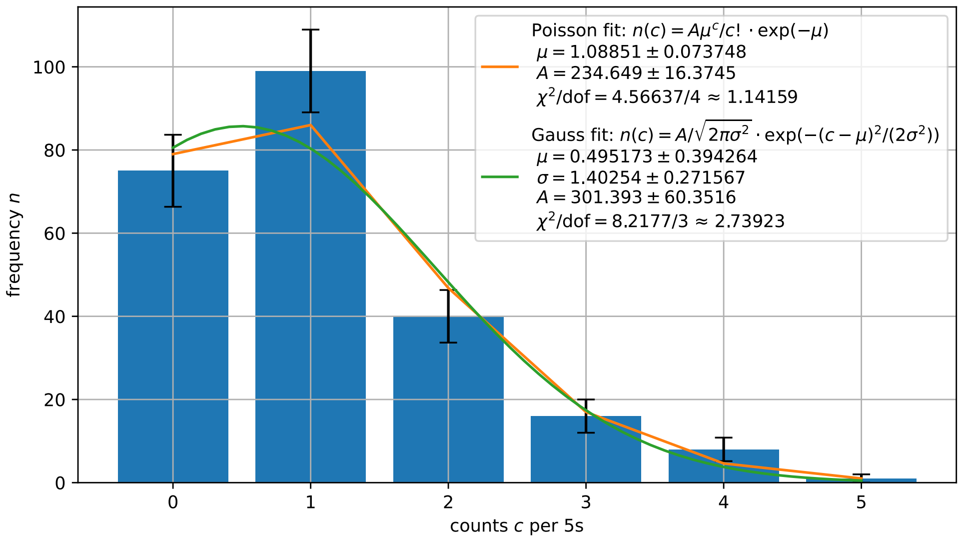

Figure 3: Probability distribution of the coincidence counts. Measured in the top floor with 239 measurements, 5s each.

In all future measurements, we will therefore assume the statistical uncertainty on the number N of events detected to be $\sqrt{N}$, corresponding to a Poisson distribution.

According to the scintillator data sheet [Edub], the detectors work with a detection efficiency of 99%, leading to a systematic error of 1% on the number of detected events N. This is, however, negligible in comparison to the much higher statistical uncertainty.

3.2 Analysis: Random Coincidences

When working in coincidence mode, such events are recorded separately which result in both of the detector tiles firing within a short time span, which is determined by the electronic settings of the detector. This improves the signal to noise-to-noise ratio significantly, by getting rid of a large number of spurious and background events, which have nothing to do with the muon flux we are trying to measure. However, it is to be expected that random coincidences occur as well and it is important to know how high the expected rate of such is, in order to be able to subtract it in further measurements.

According to the lab instructions [Edua], the rate of random coincidences R_{random} is given by

$$R_{\text{random}} = 2 \cdot R_{\text{A}} \cdot R_{\text{B}} \cdot \tau, \tag{3}$$

where R_{A} and R_{B} are the rates detected in tiles A and B individually and $\tau = 700\,\text{ns}$ is given in the manual as the gate width of the coincidence unit.

We compared the rates of random coincidences obtained with this formula with the rates resulting from the measurement in which the two tiles are placed far away from each other on the table, making it extremely unlikely for a muon to actually pass through both of them. With this setup, we performed a few repeated short-time-measurements (total time $7 \times 10\,\text{min}$ and $3 \times 5\,\text{min}$, see *Tables 2* and *8* in Appendix A) in the lab and the high-rise, as well as a single longer-time-measurement (20 min) in the basement. For this analysis, though, we treat them like three long-time-measurements à 70 min, 15 min and 20 min by summing up the counts and assuming a Poisson uncertainty on the total count number. The rates are then given by

$$R = N_{\text{tot}}/t_{\text{tot}}, \ \sigma_R = \sqrt{N_{\text{tot}}}/t_{\text{tot}},$$

and we calculate

$$\tau_{\text{eff}} = \frac{R_{\text{c}}}{2 \cdot R_{\text{A}} \cdot R_{\text{B}}}, \tag{4}$$

$$\sigma_{\tau,\text{eff}} = \tau_{\text{eff}} \cdot \sqrt{\left(\frac{\sigma_c}{R_c}\right)^2 + \left(\frac{\sigma_A}{R_A}\right)^2 + \left(\frac{\sigma_B}{R_B}\right)^2},$$

which turns out to be several orders of magnitude higher than the τ given in the instructions.

The exact values vary for the three chosen locations:

$$\tau_{\text{eff, highrise}} = 2.2(6) \cdot 10^{-4}\,\text{s}$$
$$\tau_{\text{eff, lab}} = 6(2) \cdot 10^{-5}\,\text{s}$$
$$\tau_{\text{eff, basement}} = 7(5) \cdot 10^{-5}\,\text{s}$$

This at the first look surprising finding can be explained by taking into account the showers of particles created between the point in the atmosphere where primary cosmic radiation first interacts and the point at which muons are created in the decay of pions. Muons themselves do dot cause further cascading, as they hardly interact electromagnetically. If two muons coming from different "branches" of the particles showers hit the detector tiles placed at a distance from each other, they will create a coincidence detected in the setup. Even though such two muons are not completely unrelated, we need to take them into account as a second source for random coincidences.

Assuming the influence of showers to be about the same across the area of the tiles, we use a modified version of the above given formula eq. (3) for the random coincidence rate, substituting τ for τ_{eff}. Furthermore, we make the simplifying assumption, that R_{random} does not show an additional dependence of the detector angles.

In all further data analysis, we calculate the corrected rate R of events detected from the measured value $R_{\mathrm{meas}} = \frac{N}{t}$ via:

$$R = R_{\mathrm{meas}} - 2 \cdot R_{\mathrm{A}} \cdot R_{\mathrm{B}} \cdot \tau_{\mathrm{eff}}. \tag{5}$$

The corresponding uncertainty is calculated using the following error propagation:

$$\sigma_{\mathrm{R}} = \sqrt{\sigma_{\mathrm{meas}}^2 + (2\,\sigma_{\mathrm{A}}\,R_{\mathrm{B}}\,\tau_{\mathrm{eff}})^2 + (2\,R_{\mathrm{A}}\,\sigma_{\mathrm{B}}\,\tau_{\mathrm{eff}})^2 + (2\,R_{\mathrm{A}}\,R_{\mathrm{B}}\,\sigma_{\tau,\mathrm{eff}})^2}.$$

3.3 Analysis: Zenith Angle Dependence of Muon Flux

For each chosen angle Θ, the number of coincidences N_{C} as well as the number of events detected in the individual tiles N_{A} and N_{B} during the time span t are recorded and the corrected coincidence rates R are calculated as described in the above paragraph. The statistical uncertainty on the angle Θ is estimated taking into account the precision with which the scale on the telescope arm can be read off and assuming a triangular distribution:

$$\sigma_{\theta} = \frac{0.5\,^{\circ}}{\sqrt{6}} \approx 0.2\,^{\circ}.$$

In order to eliminate any systematic error on the angle Θ as far as possible, a spirit level is used to precisely align the telescope arm and the two detector tiles before the start of any measurement.

The flux Φ of muons is given by

$$\Phi = \frac{R}{a^2 \cdot \Omega}, \tag{6}$$

where R is the rate of coincidences measured, a^2 is the area of the detector and Ω the solid angle between the two tiles. The dimensions of the scintillator are given in the manual [Edua] as 15 x 15 x 1 cm, with $a = 15\,\mathrm{cm}$ being the side length of the rectangle. We assume the uncertainty on a to be negligible.
The solid angel Ω depends crucially on the distance d between the two detector tiles, which is why this distance is chosen and measured carefully each time when the muon telescope is assembled for a new measurement.

We do not know where exactly in the casing the scintillator tiles are positioned. Assuming the two tiles to be identical in structure, we measure d from the top of the upper detector tile to the bottom of the lower detector tile, as shown in fig. 1. Using this method should prevent a systematic error on d due to the unknown exact position. The distance d was measured using a ruler with a millimetre scale division, from which a statistical uncertainty of

$$\sigma_{\mathrm{d,\ stat1}} = \frac{0.5}{\sqrt{6}}\,\mathrm{mm}$$

results. Additionally, we need to take into account that the scintillators both have a thickness of 1 cm, which gives us another statistical uncertainty component, as the detection can happen anywhere within the thickness of the detector materials:

$$\sigma_{\mathrm{d,\ stat2}} = \frac{1}{\sqrt{6}}\,\mathrm{cm} \approx 0.4\,\mathrm{cm}$$

As this second component is much larger, we can neglect the first one and simply assume a statistical uncertainty of 0.4 cm on all distances d.

In [Mat22], a formula is given for the solid angle that spans from the centre of the lower tile:

$$\Omega_{\mathrm{centre}}(a, d) = 4 \cdot \arctan\left(\frac{a^2}{4\,d\,\sqrt{1 + 2\,(\frac{a}{2\,d})^2}}\right). \tag{7}$$

We use the graphs given in [Advb]. From the right graph one can see that for $a/d \leq 0.3$, the deviation between the integrated curve over all positions and the centre curve is less than 2 %. We take this into account when choosing the distance d in all of the measurements and make sure that this is fulfilled, so that we can use the above given formula as an acceptable approximation for calculating the solid angle Ω.

The statistical uncertainty on d propagates into a statistical uncertainty on Ω as follows:

$$\sigma_{\Omega,\mathrm{stat}} = \frac{8\,a^2\,\sigma_\mathrm{d}}{(a^2+4\,d^2)\cdot d\cdot\sqrt{1+\frac{a^2}{2\,d^2}}}. \tag{8}$$

Additionally, there is a systematic uncertainty on Ω from using the "centre-formula-approximation" described above:

$$\sigma_{\Omega,\mathrm{syst}} = 0.02\cdot\Omega.$$

In our case, $\sigma_{\Omega,\mathrm{stat}}$ and $\sigma_{\Omega,\mathrm{syst}}$ are both around 10^{-3} sr. In order to be able to further propagate the error on Ω, we combine the two uncertainties into a total uncertainty:

$$\sigma_\Omega = \sqrt{\sigma^2_{\Omega,\mathrm{stat}}+\sigma^2_{\Omega,\mathrm{syst}}}.$$

From the solid angle Ω and the measured coincidence rate R, we can calculate the flux Φ through the detector using eq. (6). The uncertainty on the flux is then obtained via the following error propagation:

$$\sigma_\Phi = \Phi\cdot\sqrt{\left(\frac{\sigma_\mathrm{R}}{R}\right)^2+\left(\frac{\sigma_\Omega}{\Omega}\right)^2}$$

The exact dependence of the muon flux Φ on the zenith angle Θ is complicated, as it is given by the convolution of the creation distribution with the effects of decay and interactions [PDG18]. Near sea level, which is an acceptable simplification for our case, the angular dependence can, however, be estimated to have the shape

$$\Phi(\Theta) = A\cdot\cos^2(\Theta). \tag{9}$$

We plot the flux Φ measured as a function of the zenith angle Θ and fit functions of the form given in eq. (9) to the data points. The data points and fit results for the three locations are given in fig. 5 - fig. 7 respectively. The legends include the best-fit values as well as the reduced χ^2 as a measure for the goodness of the fits.

3.3.1 Highrise

On the top floor of the physics highrise, the zenith angle measurement was performed at a corner of the building, with glass at two sides and thus a fairly symmetric shielding on both sides of the setup (see fig. 4). As one can see in fig. 5, the data points follow the expected $\cos^2$ behaviour quite well within the limit of their uncertainties. The fit parameter A is a measure of the total flux at this location, which can already roughly be compared to the values for the other two locations. We will later see that it is in fact directly proportional to the integrated flux through the positive semi-sphere.

3.3.2 First Floor Lab

The data from the first floor lab, as shown in fig. 6, show a clear asymmetry, with the flux at negative angles tending to be higher than the flux at the respective positive angles. The geometry of the laboratory brings about a much more asymmetric shielding than the setup on the first floor, with a wall on one side and a big window on the other side of the muon telescope. We defined positive angles as the direction in which the upper tile was moving away from the window and thus facing the inside of the building. It thus makes absolute sense that the flux is lowered on this side.

Furthermore, the amplitude A in the fit is also lowered in comparison to the measurement on the lop floor, corresponding to a lower overall flux.

Figure 4: Setup of the muon telescope on the top floor of the physics highrise.

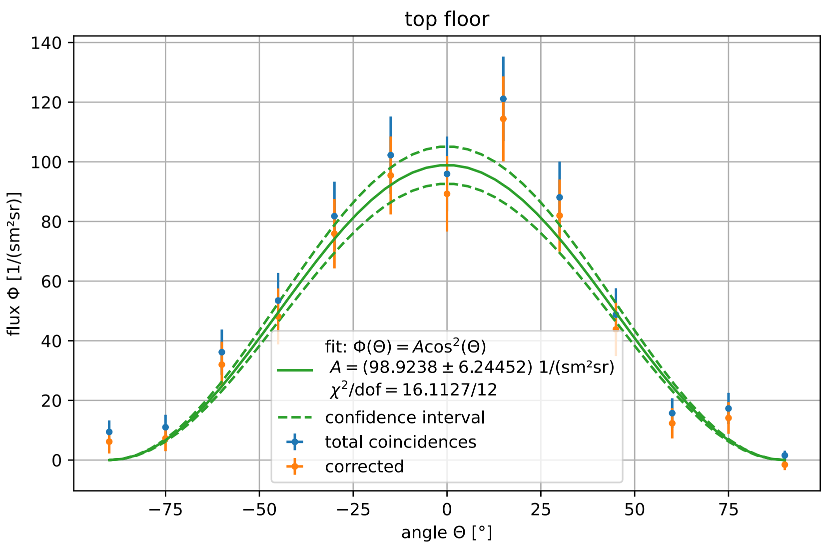

Figure 5: Angular distribution of the muon flux (coincidences versus zenith angle) with a $\cos^2\Theta$ fit. The uncertainties on the flux have been considered in the fit, but not the uncertainties on the angle Θ, which are also too small to be visible.

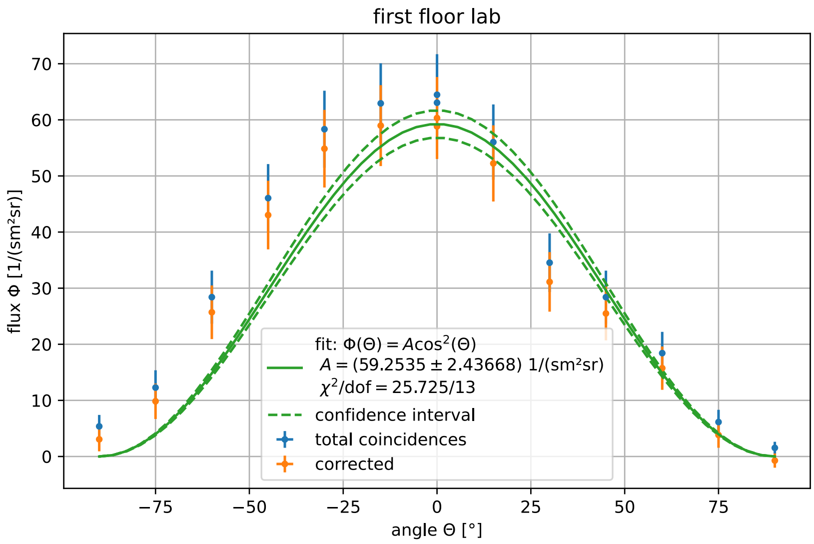

Figure 6: Angular distribution of the muon flux (coincidences versus zenith angle) with a $\cos^2\Theta$ fit. The uncertainties on the flux have been considered in the fit, but not the uncertainties on the angle Θ, which are also too small to be visible.

The two results for the vertical orientation $\Theta = 0^\circ$ are:

$$\text{short-time-measurement (10min):}\ \Phi(0^\circ) = (63 \pm 7)\frac{1}{\text{s m}^2\text{ sr}}$$
$$\text{long-time-measurement (12h):}\ \Phi(0^\circ) = (61.9 \pm 1.4)\frac{1}{\text{s m}^2\text{ sr}},$$

so as expected, they are well compatible with each other, but the long measurement results in a much lower uncertainty. Looking at the error contributions to the flux, we noted that the flux uncertainties are all dominated by the Poisson count uncertainty, whereas the contribution of σ_Ω is multiple orders of magnitude lower at $\sim 10^{-5}$ sr. This also indicates that the statistical part of σ_Ω is essentially negligible, and the systematic part also has only an influence of around 10^{-5} sr on the fit results.

3.3.3 Basement

In the basement we took less measurements due to the fact that each measurement took longer to account for the overall reduced flux. This lower flux is also reflected in the value of the amplitude A resulting from the fit in fig. 7. The reduced χ^2 is also highest in this case, in consistency with the visually reduced quality of the fit. Still, the rough $\cos^2$ shape can be seen.

3.4 Analysis: Flux Through Horizontal Detector

There are three ways to calculate the mean muon flux $\hat{\Phi}$ through each of the detectors. First, we can just use the counts $N_{A,B}$ that the detectors measured in a certain time and calculate

$$\hat{\Phi}_{A,B} = \frac{N_{A,B}}{t\,a^2\,2\pi}. \tag{10}$$

Specifically, we use the values $N_{A,B}(0^\circ)$ from the zenith-angle-measurement for each of the three locations. In the laboratory, we have one short (10 min) and one long-time measurement (12 h), and we only use the value from the long-time measurement here. The statistic uncertainty is again given by a Poisson-error:

$$\sigma_{\hat{\Phi}} = \frac{\sqrt{N_{A,B}}}{t\,a^2\,2\pi}.$$

The resulting values $\hat{\Phi}$ are given in the first and second row of table 1.

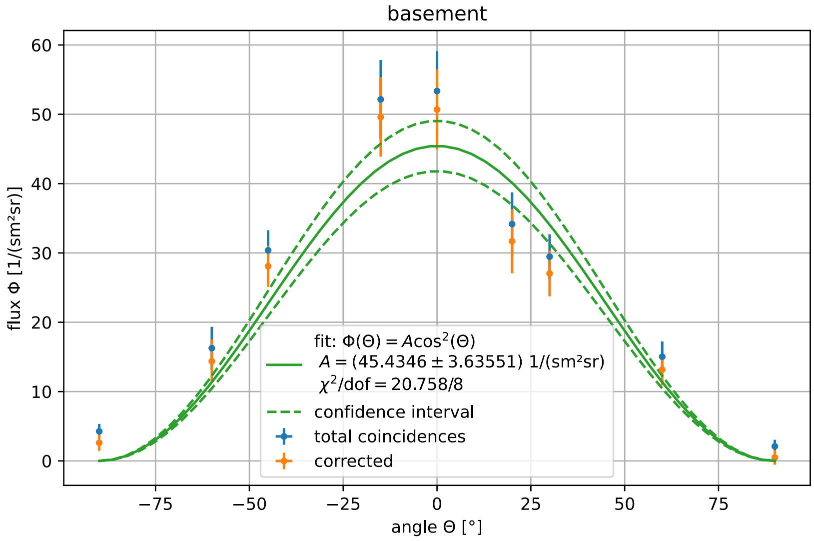

Figure 7: Angular distribution of the muon flux (coincidences versus zenith angle) with a $\cos^2\Theta$ fit.The uncertainties on the flux have been considered in the fit, but not the uncertainties on the angle Θ, which are also too small to be visible.

Another method to determine $\hat{\Phi}$ is to use the coincidence flux measured in section 3.3 at different angles, assume rotational symmetry around the vertical axis and integrate over the solid angles in the upper half sphere Ω_+:

$$\begin{aligned}\hat{\Phi} &= \frac{1}{\Omega_+}\int_{\Omega_+}\Phi(\Theta)d\Omega = \frac{1}{2\pi}\int_0^{2\pi}\int_0^{\pi/2}\Phi(\Theta)\sin(\Theta)d\Theta d\phi \\ &= \int_0^{\pi/2}\Phi(\Theta)\sin(\Theta)d\Theta = \int_0^{\pi/2} A\cos(\Theta)^2\sin(\Theta)d\Theta = A/3\end{aligned} \tag{11}$$

with the amplitude A determined in the fits of section 3.3. The results from this calculation are given in the third row of table 1.

Finally, in the high-rise, we also performed an additional measurement of the coincidence flux at varying detector distances that we can extrapolate to the distance $d = 0\,\mathrm{m}$:

$$\hat{\Phi} = \lim_{d\to 0}\Phi_{\text{coincidence}}. \tag{12}$$

Since we had to measure at small distances d, we can't use the large-distance-approximation for the solid angle that we have used before. Instead, we determine Ω from the plot in [Advb], that is, we read the values for each individual distance off from the plot. Additionally to the measurement uncertainty of d, this produces a statistical uncertainty in reading the plot that we assume to be around $\sigma_{\text{read}} \approx 0.01\,\mathrm{sr}$. For the uncertainty contribution of d, we use the centre-approximation-formula from before (eq. (8)) as an approximation. The total statistic uncertainty is then calculated via

$$\sigma_\Omega = \sqrt{\sigma_{\text{read}}^2 + \sigma_{\text{stat}}^2},$$

where the contribution σ_{stat} is nearly negligible for large distances ($\sim 10^{-3}\,\mathrm{sr}$ at $d \approx 48\,\mathrm{cm}$), but becomes dominant at small distance ($\sim 0.1\,\mathrm{sr}$ at $d \approx 8\,\mathrm{cm}$).

The flux is then calculated like before in eqs. (5) and (6). The resulting plot is shown in fig. 8.

Even though the statistical uncertainties are rather large, it is visible that with decreasing distance, the flux also decreases. For small distances, it should converge to the single detector flux $\hat{\Phi}$. The data converge approximately to a linear decrease in the small-distance-range $d < 0.3\,\mathrm{m}$. We therefore perform a linear fit $\Phi = a\,d + b$ in this interval and use the resulting optimal parameter $b = (41 \pm 11)\frac{1}{\mathrm{s\ m^2\ sr}}$ as an estimation for $\hat{\Phi}$.

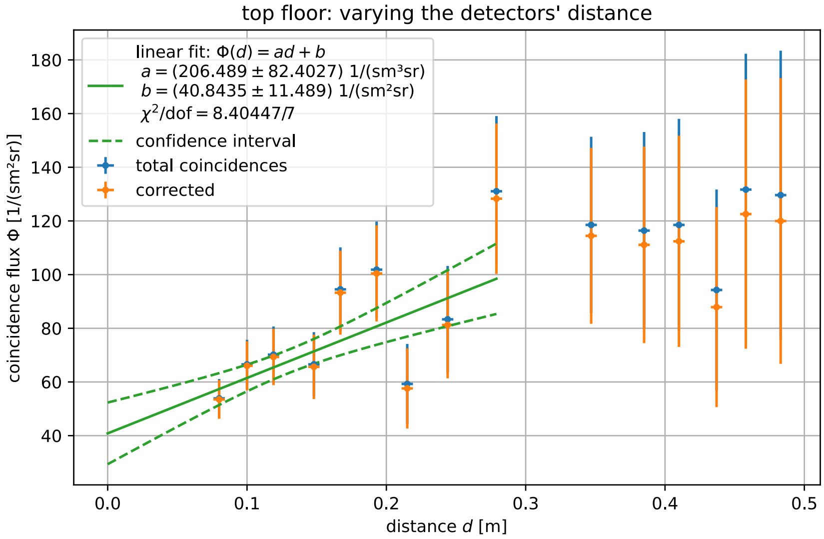

Figure 8: Coincidence flux at $\Theta = 0^\circ$ for different distances between the detectors. A linear fit was performed on the values at $d < 0.3\,\mathrm{m}$, taking into account the uncertainties on the flux, but not the uncertainties on d.

$\hat{\Phi}$ [1/(s m² sr)]	top floor	first floor	basement
single detector A	40.6 ± 1.0	32.92 ± 0.07	26.2 ± 0.5
single detector B	39.7 ± 1.0	31.66 ± 0.07	24.1 ± 0.5
coincidence integral	33 ± 2	19.8 ± 0.8	15.1 ± 1.2
coincidence extrapolation	41 ± 11		

Table 1: Results for the flux $\hat{\Phi}$ through a horizontal detector, calculated with different methods (eqs. (10) to (12)) and for different places in the building.

3.5 Analysis: Shielding Effect of Lead

In this part of the experiment, we placed different amounts of lead blocks on a table between the two detector tiles and measured the rate of coinciding events. A picture of this setup can be found in fig. 9, the measured data are listed in *Table 4* in Appendix A.

The lead blocks were placed on a foam cushion in order to accommodate for the height difference towards the base at which the telescope arm was fixed. The thickness L of the heap of lead blocks was measured using a ruler. The statistical uncertainty resulting from how precise it was possible to determine this thickness was estimated with a triangular distribution:

$$\sigma_\mathrm{L} = \frac{1.5}{\sqrt{6}}\,\mathrm{mm} \approx 0.6\,\mathrm{mm}$$

The flux is again calculated from the corrected coincidence rates like in the previous analysis parts. The resulting values Φ are plotted against the lead thickness L in fig. 10. One can see that there is a general tendency for the flux to decrease for increasing L, but there is a great deal of fluctuations and it is hard to see a clear pattern.

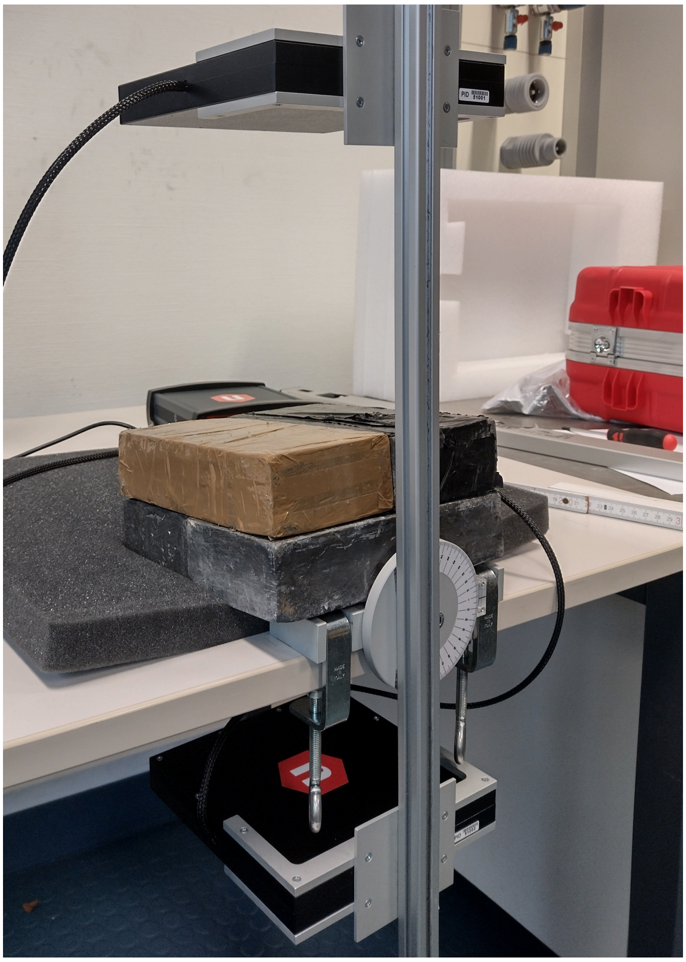

Figure 9: Setup for the measurement of the absorption in lead

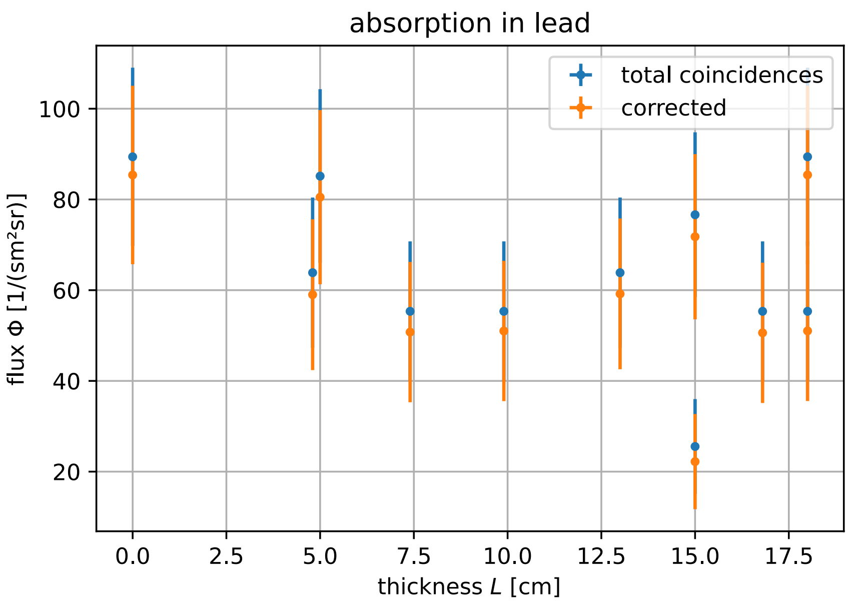

Figure 10: Measured flux through lead blocks of different thickness.

4 Discussion

4.1 Discussion: Probability Distribution

In the first part of this series of experiments, we investigated the underlying probability distribution behind the detection of cosmic muon by repeatedly measuring the number of coincidences in the muon telescope within a short time interval. This was conducted twice with different integration times. The main takeaway from this part is probably the insight of how important it is to choose a sensible integration time. Upon first choosing a time interval of 1 min, the number of detected events was so high that the obtained histogram had already transitioned quite far into the direction of a Gaussian curve. Only by choosing a much shorter integration time were we able to confirm the expected Poisson distribution character of the muon detection. This nicely illustrates the different realms of application of the two discussed distributions and how a Gaussian distribution can be seen a limit case of a Poisson distribution for high event rates .
In order to obtain an even higher statistical significance, it would have been advantageous to sample even more data. This might have further improved the fit quality.
Another point worth discussing is the question of which range should be considered in the fit. In fig. 3 for instance, one can see that during the chosen time span of 5 s, we obtained a few time 0, 1, 2, 3, 4, or 5 coincidences respectively, but never 6 or more. Theoretically, one would need to take all those higher numbers (with a respective bin count of 0) also into account when performing the fit, which was neglected in this work.
Similarly, it is a bit questionable how correct the choice of assigning the number of counts in each bin a Poisson distribution is. Even though this is the standard procedure, it seems a bit illogical to take into account a Poison error in performing both the Gaussian and the Poisson fits, when the aim is to confirm the underlying probability distribution.

4.2 Discussion: Random Coincidences

By measuring the rate of coincidences and single tile events for a detector configuration in which the two detector tiles lie at a distance from each other, we were able to find out that the formula eq. (3) as given in the manual [Edua] was not actually accurate, as it does not take into account the effect that muons from different branches of a shower are reaching the detector at the same time. From the performed measurements a new effective factor τ_{eff} was calculated and used in all subsequent data analysis to correct the obtained muon rates for the expected rate of random (and shower) coincidences.
Interestingly, this τ_{eff} was found to vary significantly for the three different locations at which the experiment was conducted. The reasons for this are not quite clear to us, as it makes little sense that the effect of showers should be so strongly dependant on the shielding or the altitude. One would expect most of the showers to emerge at a large distance above ground and as soon as pions have decayed into muons there should not be much new shower behaviour emerging, as muons hardly interact electromagnetically. One possible explanation for the observed differences might be different rates of background radiation (from the walls or other experiments in the lab) at the different locations. As we did not investigate this any further, this is therefore only a speculation. The occurrence of showers and how they are affected by the location of the experiment is something that would definitely be an interesting topic for further experiments.

Something that was however not taken into account here, due to the limited resources and time, is the angular dependence of the rate of random coincidences, which was simply assumed to be proportional to the product of the detected rates R_{A} and R_{B} at any given angle. If one was interested in taking such a potential additional dependence into account as well, one could for example repeat the measurement with the two separated tiles and fix them on a board which can be tilted.

4.3 Discussion: Zenith Angle Dependence on Muon Flux

In this part of the experiment, we examined the dependence of the muon flux on the zenith angle Θ, taking into account the geometry of the setup in the form of the scintillator tile area and the solid angle between the two detector tiles. This experiment was performed at three different locations and in all three cases, functions of the form

$$\Phi(\Theta) = A \cdot \cos^2(\Theta)$$

were fitted to the data points, in accordance with the theoretical expectations (see figs. 5 to 7). As mentioned before, the data points showed varying degrees of asymmetry and goodness of fit, depending on the location in which the data was taken. This is mainly due to the different amounts of shielding that the setup was surrounded by. The curve looks smoothest and has the highest amplitude A for the measurements performed on the top floor of the highrise.

It is worth pointing out that we did not take into account any angular dependence in the $\phi-$direction into the fit. According to theoretical considerations (compare e.g. [PDG18]), such a dependence is assumed to be negligible close to the surface of the earth, but in our case the asymmetric shielding in the different rooms makes it obvious that this is not the case. If we were able to redo the measurement on a day with great weather, it would be advisable to actually do it outside and as far from shielding influences as possible. Alternatively, one could repeat the whole experiment several times and rotate the whole setup between each execution to get a handle on the rotational symmetry.

We can try to estimate the amount by which the flux is expected to decrease after passing through the amount of material between the highrise location and the basement location, in the extreme case. Taking into account the plan of the building [Adva] provided on Ilias, we make the rough estimation that the basement location is shielded by 2.4 m of standard rock (or concrete) in vertical direction. Assuming the average energy of muons reaching us to be 4 GeV [PDG18], we obtain a range of around $r = 8$ m, using the CSDA range and density given in [PDG10]. If we now assume the amplitude A_{high} to be proportional to the total flux we measured on the top floor, assume that it is approximately the same as the unshielded flux, and make the simplifying assumption that the reduction of flux happens linearly as a function of shielding depth x, we can write

$$A(x) = A_{\text{high}} - \frac{A_{\text{high}}}{r} \cdot x$$

which yields us

$$A_{\text{base, expected}}(x = 2.4\,\text{m}) \approx 70\,\frac{1}{s\,m^2\,sr},$$

which is in fact quite a bit more than the actually obtained amplitude for the basement from the fit in fig. 7 of around $45(4)\,\frac{1}{s\,m^2\,sr}$.

It is not very surprising that the above described rough estimation did not produce a value that is actually compatible with the experimental value, as we did some considerable simplifications. One of the most significant simplifications is the fact that we only considered one mean muon energy. In reality, cosmic muons reach the earth with a very wide range of energies, even up to a few TeV, which is also the reason why it is so hard to shield them away completely and why many big scale particle physics experiments are located many kilometres deep under ground.
Secondly, we might have underestimated the amount of material above the basement location, or miss-interpreted it as standard rock. Potentially higher concentrations of more strongly absorbing materials, like certain metals, might have been present as well. The amount of shielding is also different for different angles and tends to be higher for larger zenith angles, which means that the fit amplitude possibly underestimates the actual vertical flux. Similarly, the assumption of a linear decrease might have been to strong of a simplification.
Finally, the amplitudes obtained in the fits might not have been as accurate as possible, due to the limited time spend on each measurement. Performing longer measurements and at more finely spaced angles might help to improve the experimental results.

4.4 Discussion: Flux Through Horizontal Detector

We have estimated the flux through a single horizontal detector with three different methods. Results are given in table 1. For all of the locations where we performed measurements, the first method (based on the total event rate at one of the detectors, eq. (10)) gave significantly larger results than the second method (based on the solid-angle-integral over the coincidence flux, eq. (11)). This difference was expected since the first method doesn't exclude internal noise in the detector - accidental discharges that were not induced by a particle and that are thus not present in the coincidence measurements. Furthermore, since the detector efficiency ϵ is not exactly 100%, the combined efficiency ϵ^2 of both scintillators in the coincidence measurement is slightly decreased compared to the single tile efficiency. Finally, it is also possible that a small fraction of the incoming muons get fully absorbed, get scattered or lose enough energy in the first detector that they can not be detected by the second detector anymore, which will further decrease the coincidence flux.

This last effect could also be one reason for the difference between the different detectors A (which was always above) and B (below): In the results of method 1, detector A always has a slightly larger flux than B. We do not know for certain, though, whether this difference does indeed depend on the positioning of the detectors or whether it is an inherent difference between the two scintillators. For example, detector A could be more sensitive to low energy particles or to electric noise. This question could potentially be examined in another experiment by exchanging the detector positions.

The extrapolation of coincidence flux at small distances (method 3, eq. (12)) gives approximately the same values as the first method, but it has a large statistical uncertainty ($\sigma_{\hat{\Phi}}/\hat{\Phi} \approx 27\%$) and is hence not significantly deviating from any of the other top-floor-results. This statistical uncertainty is mainly originating from the Poisson uncertainty on the coincidence counts, as we can see comparing the error contributions throughout the error propagation. Besides, we have a potentially important systematic error from the fact that we have assumed and fitted a simple linear extrapolation line. Longer measurement times and measuring at smaller distances would enable us to choose a more suitable fit function and perform a better fit.

Finally, we can compare the results at different places in the building: As expected, the highest flux was measured in the top floor and the lowest in the basement. This is true for each of the employed methods.

4.5 Discussion: Shielding Effect of Lead

As lead is a material with a high atomic number and density, which is known for strongly absorbing particles, one would in general expect the flux to decrease when increasing the thickness of lead shielding. This effect is only as a rough tendency visible in fig. 10. There are several possible explanations for why this might be the case.
One idea is that the amount of lead piled up in this experiment was simply not thick enough to result in a significant shielding of the muon flux. We can make a rough estimation of the range of muons in lead using the *Continuous Slowing Down Approximation (CSDA)* and the values given in [PDG16]. Assuming the mean energy of muons reaching the lab to be 4 GeV (compare [PDG18]), the CSDA range is approximately

$$2.946 \cdot 10^3, \frac{\mathrm{g}}{\mathrm{cm}^2}$$

and with an average density of $11.350\,\frac{g}{\mathrm{cm}^3}$ [DNS01] this corresponds to a range of approximately

$$2.6\,\mathrm{m}.$$

Even though this is obviously only a rough estimation as the actual energy distribution of the muons is not known to us, it indicates that the layer of lead shielding of maximum 18 cm was indeed not enough to significantly dampen the muon flux. A second aspect to consider is the fact that the experimental setup was not exactly ideal for investigating the shielding of radiation, as the lead blocks were only placed central on top of one of the detector tiles and nothing prevented radiation from entering the telescope at a slight angle or next to the lead blocks, which did not cover the whole detector surface. If one were to repeat the experiment, it would be advisable to come up with a way of actually covering the full surface of the detector with lead and to do so as evenly as possible. In the here performed experiment it was also an issue that the lead blocks were not lying completely flat, thus leaving air between them and making it hard to measure their thickness overall. Besides, it would be better to use a much larger volume of lead in general, in order to obtain a more significant effect. In order to obtain a better statistical significance and to take into account the fluctuations in the measured flux, repeated and longer measurements would have been necessary.

Another factor that we only indirectly took into account is the altitude. In order to obtain reliable measurements on the effect of the altitude on the muon flux, one would, however, need to eliminate the problem of having different degrees of shielding in different locations and to include larger altitude differences. One idea for how this could be realised would be to use a hot air balloon or other airborne vessel.

5 Conclusion

This series of experiments was dedicated to measuring the flux Φ of cosmic muons at different locations, with different degrees of shielding, different detector configurations and at different zenith angles Θ.
In a preparatory experiment, the nature of the probability distribution governing the detection of muons was investigated. It was confirmed that this process can indeed be modelled as a Poisson distributed, but it was also observed how this transitions into a Gaussian distribution for larger event rates.
Secondly, measurements were performed to get an estimation on the expected rate of random coincidences. The effect of showers of particles creating semi-random coincidences was observed and discussed and a correction to the originally assumed linear relationship between the rate of random coincidences and the product between the single tile rates $R_{A,B}$ was calculated. All experimentally obtained rates were corrected for random coincidences via

$$R = R_{\mathrm{mess}} - 2\, R_{\mathrm{A}}\, R_{\mathrm{B}}\, \tau_{\mathrm{eff}}.$$

In the third part of the experiment, the flux Φ through the detector was measured as a function of zenith angle Θ and the resulting data was fitted with functions of the form

$$\Phi(\Theta) = A \cdot \cos^2(\Theta)$$

in accordance with the theoretical expectation. The difference in the asymmetry of the results obtained for the different locations was discussed, as well as the different amplitudes as a result of the varying amount of shielding present at the locations.

Based on these previous measurements and with an additional measurement series, we used and compared three methods to determine the mean flux through a horizontal detector. Between the methods, there were significant deviations for which we offered several explanations, but they all follow the expectation that the flux is highest in the top floor of the high-rise and lowest in the basement, reflecting the shielding from the building.

In a final series of measurements, lead blocks of different thickness were brought between the two detector tiles and the effect on the measured flux was observed. This did, however, not result in any significant change apart from a tendency to decrease with increasing lead thickness. Some reasons for this and potential for improvement were discussed.

References

[Adva] AdvLab. *Map Building*. available as PDF uploaded on Ilias. URL: https://ilias.uni-freiburg.de/ilias.php?baseClass=ilrepositorygui&cmd=sendfile&ref_id=3572085.

[Advb] AdvLab. *Solid Angle Sketch and Plot*. available as PDF uploaded on Ilias. URL: https://ilias.uni-freiburg.de/ilias.php?baseClass=ilrepositorygui&cmd=sendfile&ref_id=3572918.

[DNS01] D.E.Groom, N.V.Mokhov, and S.Striganov. *Muon Stopping Power And Range Tables*. available as PDF uploaded on Ilias. 2001. URL: https://ilias.uni-freiburg.de/ilias.php?baseClass=ilrepositorygui&cmd=sendfile&ref_id=3555607.

[Edua] CAEN Educational. *SP5620CH Cosmic Hunter QuickStart Guide*. available as PDF uploaded on Ilias. URL: https://ilias.uni-freiburg.de/ilias.php?baseClass=ilrepositorygui&cmd=sendfile&ref_id=3555604.

[Edub] CAEN Educational. *Szintillator Calibration*. available as PDF uploaded on Ilias. URL: https://ilias.uni-freiburg.de/ilias.php?baseClass=ilrepositorygui&cmd=sendfile&ref_id=3555605.

[Mat22] Richard J. Mathar. *Solid Angle of a Rectangular Plate*. available as PDF uploaded on Ilias. 2022. URL: https://ilias.uni-freiburg.de/ilias.php?baseClass=ilrepositorygui&cmd=sendfile&ref_id=3558530.

[PDG10] PDG. *Muons in standard rock*. available online. 2010. URL: https://pdg.lbl.gov/2010/AtomicNuclearProperties/MUON_ELOSS_TABLES/muonloss_281.pdf.

[PDG16] PDG. *Muons in lead (Pb)*. available online. 2016. URL: https://pdg.lbl.gov/2016/AtomicNuclearProperties/MUE/muE%5C_lead%5C_Pb.pdf.

[PDG18] PDG. *Cosmic Rays*. available as PDF uploaded on Ilias. 2018. URL: https://ilias.uni-freiburg.de/ilias.php?baseClass=ilrepositorygui&cmd=sendfile&ref_id=3555606.

6 Appendix A: Signed Lab Notes

Kosmische Myonen

16.09.24

[redacted]

Assistant : [redacted]

0) Preparations

- mounted two tiles on telescope arm
- chosen distance : $d = 61.8$ cm

  measured from top of top tile to top of bottom tile

  uncertainties :
  - scale : Δ-dist with $2a = 1$mm
  - thickness of scintillator
  - assumption : same position within casing

- dimensions scintillator : $15 \times 15 \times 1$ cm^3 (manual)

see graphs : at $\frac{a}{d} \approx 0.3$ deviation of 2% — deviation from central position calculation

here : $\frac{15}{61.8} \approx 0.24$

altitude of lab : 186m

- getting to know Cosmic Hunter software
- put setup in position in which tiles are horizontal (check with spirit level)

1) Propability distribution

start 10 min measurement, read off coincidence number every ~~min~~

$\Delta t = 1$min

Table 1

N : 3, 6, 4, 9, 6, 10, 10, 6, 9, 6, 5
9, 7, 4, 5, 2, 3, 6, 4, 5, 6
7, 6, 5, 6, 7, 0, 8, 7, 5, 6
6, 8, 9, 8, 4, 3, 3, 2, 10, 2
4, 7, 5, 6, 6, 4, 4, 3,
3, 6, 1, 6, 6, 3, 8, 6, 2, 3

①

Figure 11: Labnotes Page 1

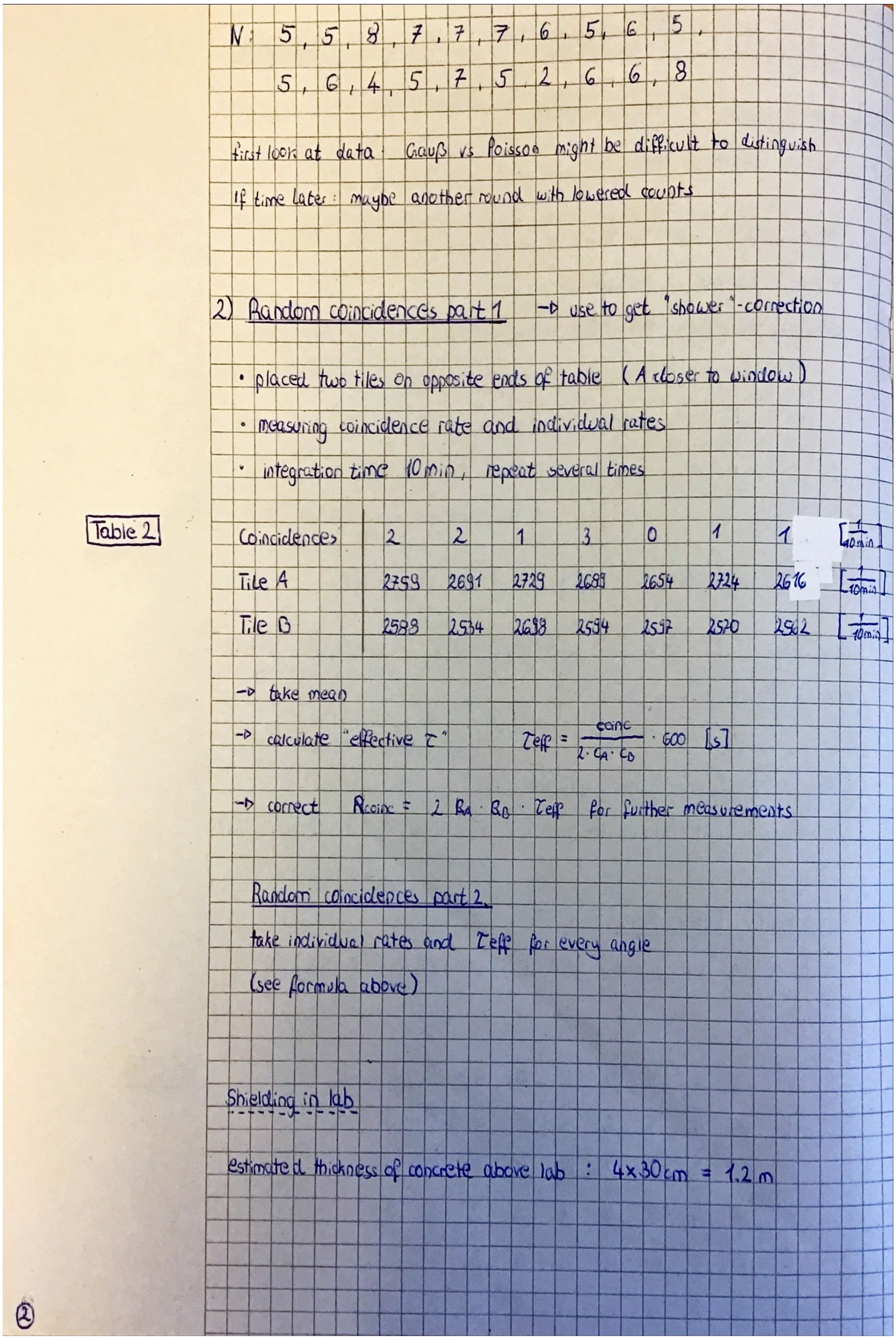

N: 5, 5, 8, 7, 7, 7, 6, 5, 6, 5,
5, 6, 4, 5, 7, 5, 2, 6, 6, 8

first look at data: Gauß vs Poisson might be difficult to distinguish
If time later: maybe another round with lowered counts

2) Random coincidences part 1 → use to get "shower"-correction

- placed two tiles on opposite ends of table (A closer to window)
- measuring coincidence rate and individual rates
- integration time 10 min, repeat several times

Table 2

Coincidences	2	2	1	3	0	1	1	$\left[\frac{1}{10\,min}\right]$
Tile A	2759	2691	2729	2689	2654	2724	2616	$\left[\frac{1}{10\,min}\right]$
Tile B	2588	2534	2698	2594	2597	2570	2562	$\left[\frac{1}{10\,min}\right]$

→ take mean
→ calculate "effective τ" $\quad \tau_{eff} = \frac{coinc}{2 \cdot c_A \cdot c_B} \cdot 600$ [s]
→ correct $R_{coinc} = 2 R_A \cdot R_B \cdot \tau_{eff}$ for further measurements

Random coincidences part 2
take individual rates and τ_{eff} for every angle
(see formula above)

Shielding in lab
estimated thickness of concrete above lab: $4 \times 30\,cm = 1.2\,m$

②

Figure 12: Labnotes Page 2

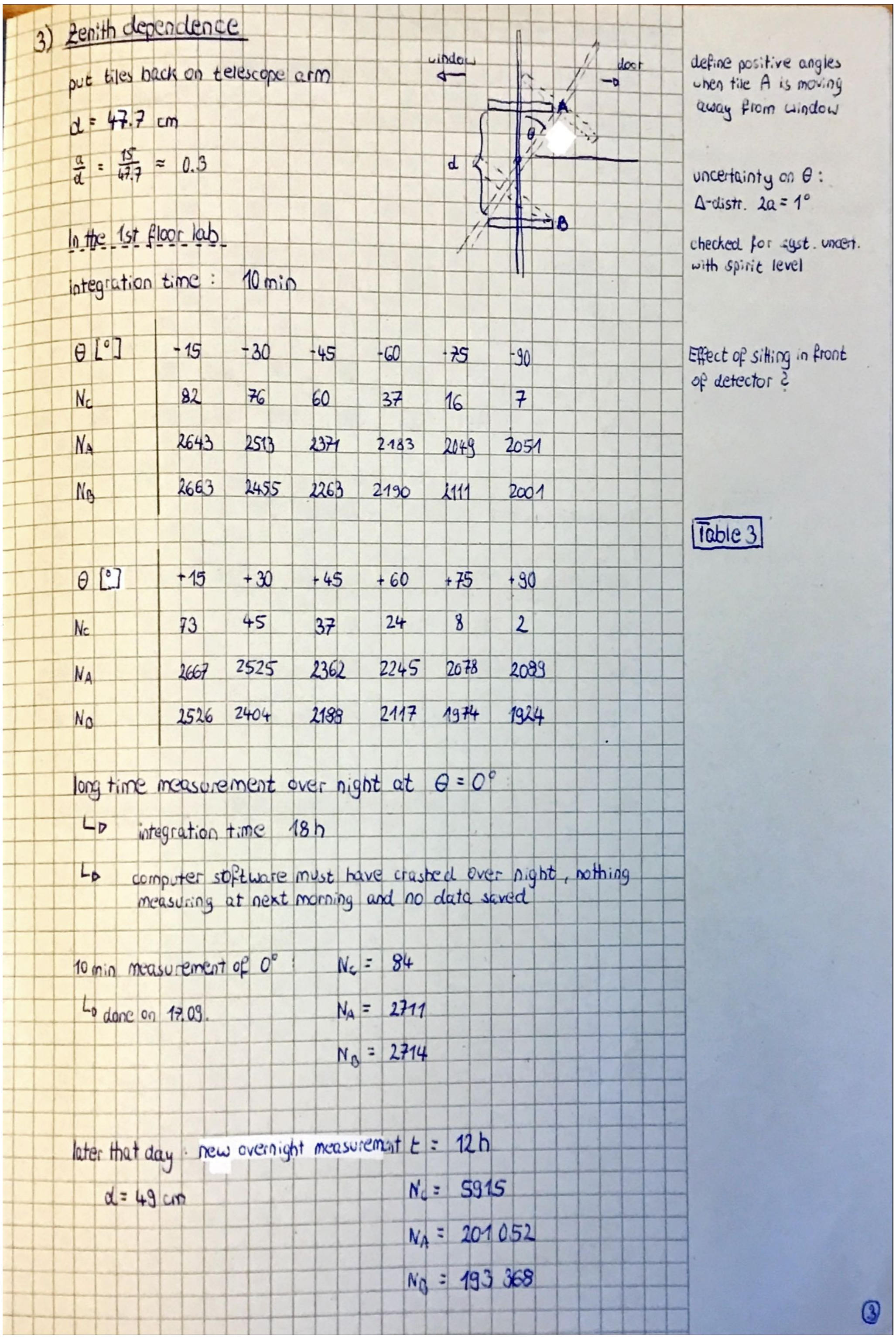

3) Zenith dependence

put tiles back on telescope arm

$d = 47.7$ cm

$\frac{a}{d} = \frac{15}{47.7} \approx 0.3$

window ← → door

A

θ

d

B

define positive angles when tile A is moving away from window

uncertainty on θ : Δ-distr. $2a = 1°$

checked for syst. uncert. with spirit level

In the 1st floor lab

integration time : 10 min

θ [°]	-15	-30	-45	-60	-75	-90
N_C	82	76	60	37	16	7
N_A	2643	2513	2371	2183	2049	2051
N_B	2663	2455	2263	2190	2111	2001

Effect of sitting in front of detector ?

Table 3

θ [°]	+15	+30	+45	+60	+75	+90
N_C	73	45	37	24	8	2
N_A	2667	2525	2362	2245	2078	2089
N_B	2526	2404	2188	2117	1974	1924

long time measurement over night at $\theta = 0°$

↳ integration time 18 h

↳ computer software must have crashed over night, nothing measuring at next morning and no data saved

10 min measurement of 0° : $N_C = 84$

↳ done on 17.09. $N_A = 2711$

$N_B = 2714$

later that day : new overnight measurement $t = 12$ h

$d = 49$ cm

$N_C = 5915$

$N_A = 201\,052$

$N_B = 193\,368$

3

Figure 13: Labnotes Page 3

Table 4

5) Shielding Effekt of lead

turned tiles around, so that table is between them

~~laptop~~ cushion for making the height even

$d = 50.3$ cm

$t = 2$ min

lead thickness [cm]	0	4.8	9.9	15	18	18	16.8	15
N_c	21	15	13	6	21	13	13	18
N_A	517	587	536	491	542	526	594	568
N_B	496	529	518	434	471	525	511	546

strange, repeat

uncertainty on lead thickness : Δ-distr. $2a = 3$ mm

lead thickness	13	7.4	5
N_c	15	13	20
N_A	589	549	564
N_B	507	534	517

note : air between lead blocks and slightly tilted setup due to weight of blocks compressing the cushion

4

Figure 14: Labnotes Page 4

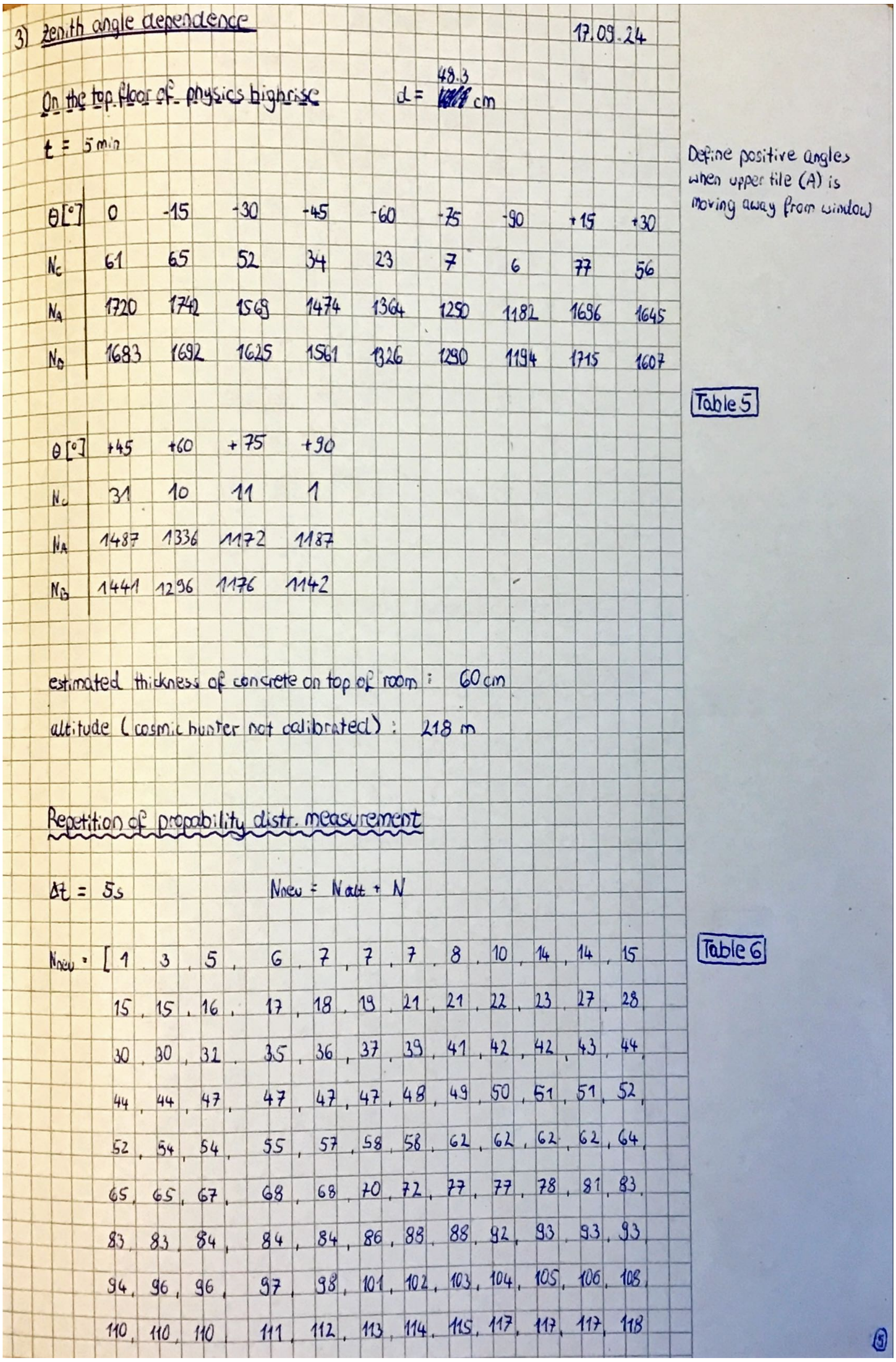

3) Zenith angle dependence 17.09.24

On the top floor of physics highrise $d = 48.3$ cm

t = 5 min

Define positive angles when upper tile (A) is moving away from window

θ [°]	0	-15	-30	-45	-60	-75	-90	+15	+30
N_C	61	65	52	34	23	7	6	77	56
N_A	1720	1742	1569	1474	1364	1250	1182	1696	1645
N_B	1683	1692	1625	1561	1326	1290	1194	1715	1607

θ [°]	+45	+60	+75	+90
N_C	31	10	11	1
N_A	1487	1336	1172	1187
N_B	1441	1296	1176	1142

Table 5

estimated thickness of concrete on top of room : 60 cm

altitude (cosmic hunter not calibrated) : 218 m

Repetition of propability distr. measurement

$\Delta t = 5s$ $N_{neu} = N_{alt} + N$

Table 6

N_{neu} = [1, 3, 5, 6, 7, 7, 7, 8, 10, 14, 14, 15,
15, 15, 16, 17, 18, 19, 21, 21, 22, 23, 27, 28,
30, 30, 32, 35, 36, 37, 39, 41, 42, 42, 43, 44,
44, 44, 47, 47, 47, 47, 48, 49, 50, 51, 51, 52,
52, 54, 54, 55, 57, 58, 58, 62, 62, 62, 62, 64,
65, 65, 67, 68, 68, 70, 72, 77, 77, 78, 81, 83,
83, 83, 84, 84, 84, 86, 88, 88, 92, 93, 93, 93,
94, 96, 96, 97, 98, 101, 102, 103, 104, 105, 106, 108,
110, 110, 110, 111, 112, 113, 114, 115, 117, 117, 117, 118

5

Figure 15: Labnotes Page 5

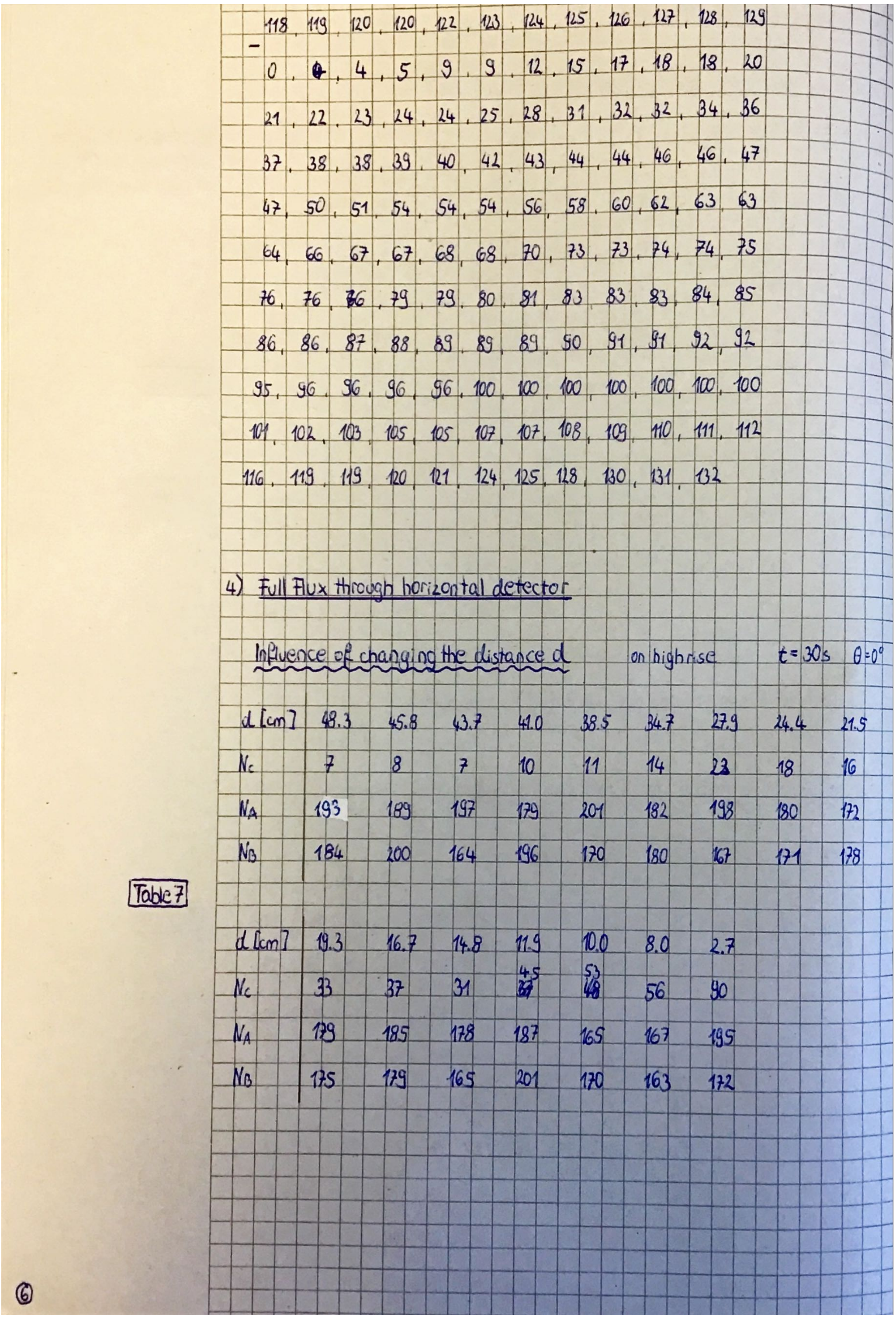

118, 119, 120, 120, 122, 123, 124, 125, 126, 127, 128, 129

–

0, [illegible], 4, 5, 9, 9, 12, 15, 17, 18, 18, 20

21, 22, 23, 24, 24, 25, 28, 31, 32, 32, 34, 36

37, 38, 38, 39, 40, 42, 43, 44, 44, 46, 46, 47

47, 50, 51, 54, 54, 54, 56, 58, 60, 62, 63, 63

64, 66, 67, 67, 68, 68, 70, 73, 73, 74, 74, 75

76, 76, [illegible], 79, 79, 80, 81, 83, 83, 83, 84, 85

86, 86, 87, 88, 89, 89, 89, 90, 91, 91, 92, 92

95, 96, 96, 96, 96, 100, 100, 100, 100, 100, 100, 100

101, 102, 103, 105, 105, 107, 107, 108, 109, 110, 111, 112

116, 119, 119, 120, 121, 124, 125, 128, 130, 131, 132

4) Full Flux through horizontal detector

Influence of changing the distance d on highrise $t = 30s$ $\theta = 0°$

d [cm]	48.3	45.8	43.7	41.0	38.5	34.7	27.9	24.4	21.5
N_C	7	8	7	10	11	14	23	18	16
N_A	193	189	197	179	201	182	198	180	172
N_B	184	200	164	196	170	180	167	171	178

Table 7

d [cm]	19.3	16.7	14.8	11.9	10.0	8.0	2.7
N_C	33	37	31	~~37~~ 45	~~48~~ 53	56	90
N_A	179	185	178	187	165	167	195
N_B	175	179	165	201	170	163	172

6

Figure 16: Labnotes Page 6

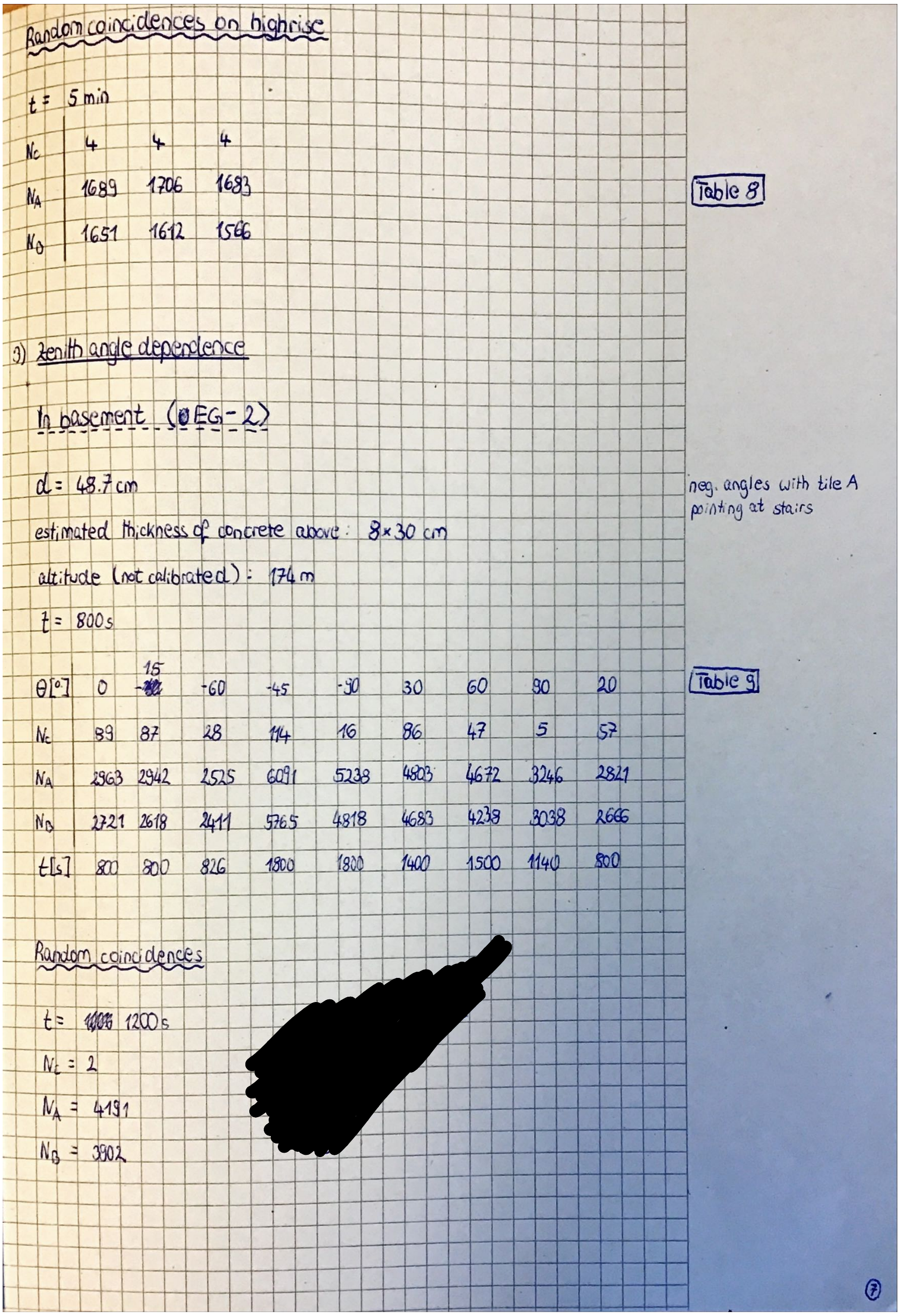

Figure 17: Labnotes Page 7